The Journal of Experimental Biology 211, 2336-2345
Published by The Company of Biologists 2008
doi:10.1242/jeb.017640

# Scaling of muscle architecture and fiber types in the rat hindlimb

Carolyn M. Eng[1], Laura H. Smallwood[1], Maria Pia Rainiero[2], Michele Lahey[1], Samuel R. Ward[2] and Richard L. Lieber[1,*]

[1]Departments of Orthopaedic Surgery and Bioengineering, University of California and Veterans Administration Medical Centers, San Diego, CA, USA and [2]Department of Radiology, University of California and Veterans Administration Medical Centers, San Diego, CA, USA

*Author for correspondence (e-mail: rlieber@ucsd.edu)

Accepted 30 April 2008

## SUMMARY

**The functional capacity of a muscle is determined by its architecture and metabolic properties. Although extensive analyses of muscle architecture and fiber type have been completed in a large number of muscles in numerous species, there have been few studies that have looked at the interrelationship of these functional parameters among muscles of a single species. Nor have the architectural properties of individual muscles been compared across species to understand scaling. This study examined muscle architecture and fiber type in the rat (*Rattus norvegicus*) hindlimb to examine each muscle's functional specialization. Discriminant analysis demonstrated that architectural properties are a greater predictor of muscle function (as defined by primary joint action and anti-gravity or non anti-gravity role) than fiber type. Architectural properties were not strictly aligned with fiber type, but when muscles were grouped according to anti-gravity *versus* non-anti-gravity function there was evidence of functional specialization. Specifically, anti-gravity muscles had a larger percentage of slow fiber type and increased muscle physiological cross-sectional area. Incongruities between a muscle's architecture and fiber type may reflect the variability of functional requirements on single muscles, especially those that cross multiple joints. Additionally, discriminant analysis and scaling of architectural variables in the hindlimb across several mammalian species was used to explore whether any functional patterns could be elucidated within single muscles or across muscle groups. Several muscles deviated from previously described muscle architecture scaling rules and there was large variability within functional groups in how muscles should be scaled with body size. This implies that functional demands placed on muscles across species should be examined on the single muscle level.**

Key words: muscle fiber type, muscle architecture, muscle mechanics, scaling.

## INTRODUCTION

Examining functional and anatomical constraints that determine muscle function provides a useful perspective for understanding how muscles are designed. The two most important design parameters that determine a muscle's functional properties are its architecture and fiber type composition (Bodine et al., 1982; Bottinelli et al., 1991; Powell et al., 1984; Reiser et al., 1985) Although ample evidence exists for the influence of architecture and fiber type on functional properties, the relationship between these two parameters has not been elucidated.

Skeletal muscle architecture is defined as the arrangement of muscle fibers relative to the axis of force generation (Gans, 1982; Lieber and Fridén, 2000). Muscle force is primarily determined by the cross-sectional area of the fibers (Powell et al., 1984), whereas muscle excursion and velocity are determined by muscle fiber length (Bodine et al., 1982). Thus the architectural features of a muscle define its functional properties. In addition to architecture, muscle fiber type influences contractile force, maximum velocity and time to fatigue (Bodine et al., 1987; Bottinelli et al., 1991; Lutz et al., 2002). The differences in contractile force between fiber types is not simply a function of differences in cross-sectional area of the fibers. Bodine et al. (Bodine et al., 1987) examined the effect of fiber type on specific tension and found significant differences between fast and slow fibers even after accounting for differences in cross-sectional area. Furthermore, there are major metabolic differences among the various fiber types. The slower fibers rely more heavily on oxidative phosphorylation and consequently have a higher mitochondrial density than the faster fibers, which are more reliant on glycolysis to metabolize glucose (Peter et al., 1972). Thus, the fiber type of a muscle is closely aligned with its metabolic properties.

Taken together, architectural properties and fiber type composition can be used to predict maximum muscle force, excursion and velocity. Since both architectural and metabolic properties affect function, it is interesting to know the extent to which they co-vary. In other words, one could ask, are muscles 'designed' to be fast-contracting, by increasing their fiber length *and* their fast fiber type percentage or do the two parameters vary independently?

The only animal for which the entire hindlimb muscle architecture and fiber type composition have been simultaneously measured is the mouse (Burkholder et al., 1994). Although the mouse model is important because of its widespread use in transgenic studies, there were two main limitations of that previous study: first, fiber types were characterized histochemically, which, although functionally and morphologically relevant, has limited use in comparing muscles of 'similar' fiber types. Histochemical assays are not specific enough to compare properties of muscle proteins across species. A second weakness was that the very small size of the mouse results in a fiber type composition that is heavily biased toward fast fibers. This limits the utility of regression analysis since a relatively narrow range of one of the independent variables (i.e. fast fiber type percentage) is

available. It is thus desirable to perform such a study in a larger, commonly studied mammalian model. The classical mammalian animal model whose muscle architectural and neurophysiological properties have been extensively described is the cat. However, the high cost, animal care and use issues, and size of tissues to be analyzed make the cat an impractical model. The rat is a good compromise because a vast amount of physiological, behavioral and morphological data already exist for this species and, although the rat hindlimb is a highly utilized model for musculoskeletal research, the architecture of only a few muscles has been defined. From a fiber-type standpoint, the rat's size is an order of magnitude greater than the mouse, making it more likely to contain a higher fraction of slow fibers. Finally, the modest rat muscle size enables full quantification without limitations due to incomplete sampling. Although several reports of fiber type distribution in portions of the rat hindlimb exist (Ariano et al., 1973; Armstrong and Phelps, 1984; Edgerton and Simpson, 1969; Pullen, 1977; Schiaffano et al., 1970; Staron et al., 1999; Staron and Pette, 1993), none have performed a comprehensive study of the entire rat hindlimb and none have correlated these data with direct architectural measurements on the same animal subjects. The one study examining both muscle architecture and fiber type composition examined only a single muscle and therefore cannot answer the same muscle design questions broached when examining functionally distinct muscles (Roy et al., 1984).

A second aspect of muscle design that provides insight into function is muscle scaling. Strong scaling relationships may reveal specific characteristics of individual muscles that exist independent of locomotor style or behavioral repertoire. Prior studies of muscle scaling across species grouped muscles according to function or anatomy (Alexander et al., 1981). Variability in muscle architecture is high within functional groups, and these studies may not reveal scaling relationships that apply to individual muscles. Additionally, most studies examining scaling of architectural variables have looked at how absolute rather than relative variables scale with body size. One study examining scaling of relative variables normalized fiber length to femur length and grouped muscles according to action (Alexander and Ker, 1990). It was concluded from this analysis that relative fiber lengths did not scale with body mass. Examination of the fiber length to muscle length ratio may reveal scaling relationships that were not elucidated in previous work.

Therefore, the purpose of this investigation was to define both the architectural features and fiber type distribution of the rat hindlimb and to compare differences in design characteristics across species.

## MATERIALS AND METHODS

Twenty-nine muscles from each of six paired hindlimbs were removed from adult male Sprague-Dawley rats (*Rattus norvegicus*; Harlan Scientific, Indianapolis, IN, USA; 323±15 g). One leg was used for analysis of fiber type distribution and the contralateral limb was used for architectural measurements. Animals were sacrificed by intracardiac injection of pentobarbital and immediately skinned and quartered. One limb was placed in 10% buffered formaldehyde within 30 min of sacrifice, with hip and knee held at 90° and ankle in neutral, and fixed overnight. Muscles from the contralateral limb were frozen in liquid nitrogen (–159°C), and stored at –80°C for subsequent fiber type analysis.

### Fiber type determination

Myosin heavy chain (MHC) isoforms were defined by SDS-PAGE as previously described (Talmadge and Roy, 1993). A myofibril-rich fraction of individual whole muscles ($N$=3 for each of 29 different muscles) was prepared and the final pellet was resuspended in sample buffer to a concentration of 0.125 mg protein $ml^{-1}$ (BCA protein assay, Pierce, Rockford, IL, USA). Total acrylamide concentration was 4% and 8% in the stacking and resolving gels, respectively (bis-acrylamide, 1:50). Gels (16×22 cm, 0.75 mm thick) were run at a constant current of 10 mA until voltage rose to 275 V, and thereafter at constant voltage for 21 h at 4–6°C. A volume of 1.25 µg total protein was loaded into a well and gels were stained with Coomassie Brilliant Blue. To ensure that adequate sensitivity was achieved for detecting minor MHC bands, each sample was also run on separate gels that were silver stained (Bio-Rad, Hercules, CA, USA). MHC bands were identified and quantified with densitometry (GS-800, Bio-Rad). The Coomassie and silver-stained gels gave similar results, so quantification results are reported exclusively from Coomassie-stained gels.

### Skeletal muscle architecture

Limbs were placed in phosphate-buffered saline (PBS) for 24–48 h after fixation to remove residual fixative. Specimens were finely dissected to isolate each of 29 muscles and were stored in PBS. Muscle specimens were removed from buffer, gently blotted dry, and weighed. Muscle length ($L'_m$) was defined as the distance from the origin of the most proximal fibers to the insertion of the most distal fibers. Fiber length ($L'_f$) was measured from three predetermined regions in each muscle using a digital caliper (accuracy, 0.01 mm). Muscle fiber bundles ($N$=3 per muscle) were carefully dissected from the proximal tendon to the distal tendon of each muscle region. Surface pennation angle was measured in each region with a standard goniometer as the angle between the fibers in each region and the distal muscle tendon. Fascicles were then placed in mild sulfuric acid solution (15% v/v) for 30 min to partially digest surrounding connective tissue, and were then rinsed in PBS. Under magnification, three small muscle fiber bundles (consisting of ~20 single fibers) were isolated from each muscle region and mounted on slides. Bundle sarcomere length ($L'_s$) was determined by laser diffraction using the zero$^{th}$- to first order diffraction angle as previously described (Lieber et al., 1990). Values for sarcomere number ($S_n$) and normalized fiber length ($L_f$) were then calculated for the isolated bundles according to the following equations:

$$S_n = \frac{L'_f}{L'_s} \quad (1)$$

and

$$L_f = L'_f \left( \frac{2.4}{L'_s} \right), \quad (2)$$

where $L'_f$ is measured fiber length, $L'_s$ is measured sarcomere length, $L_f$ is normalized muscle fiber length, and 2.4 represents the optimal sarcomere length (in µm) for rat muscle (ter Keurs et al., 1984). Normalized muscle length ($L_m$) was similarly derived. Fiber-length-to-muscle-length ratio ($L_f/L_m$) was calculated by dividing normalized fiber length by normalized muscle length.

Physiological cross-sectional area (PCSA; measured in $cm^2$) was calculated according to the following equation (Powell et al., 1984):

$$PCSA = \frac{M \cdot \cos\theta}{\rho \cdot L_f}, \quad (3)$$

where $M$ is muscle mass (in g), θ is pennation angle and ρ is muscle density (1.056 g $cm^{-3}$) (Ward and Lieber, 2005).

### Muscle groups

Muscle groups were identified based on their action about each joint. Hip flexors consisted of rectus femoris (RF) and psoas (PS), and hip extensors consisted of gluteus superficialis (GSup), gluteus medius (GMed), biceps femoris (BF), semitendinosus (ST), semimembranosus (SM) and 'muscle X'. Muscle X was a previously undescribed muscle for which no reference could be found and no homologous mammalian muscle could be defined. Its origin was the craniolateral pelvis and its insertion was the craniomedial tibia (Fig. 1). Hip adductors included adductor magnus (AddM), adductor longus (AddL), adductor tertius (AddT) and adductor brevis (AddB). Muscles in the knee flexor group were gracilis (cranial and caudal heads; GRcr and GRca, respectively), BF, ST, SM, muscle X, gastrocnemius (GLH and GMH; lateral and medial heads, respectively) and plantaris (PLA), and knee extensors included vastus intermedius (VI), vastus lateralis (VL), vastus medialis (VM) and RF. Ankle plantarflexors included GLH and GMH, PLA, soleus (SOL), tibialis posterior (TP), flexor digitorum longus (FDL) and flexor hallucis longus (FHL), and the dorsiflexors included tibialis anterior (TA), extensor digitorum longus (EDL) and extensor hallucis longus (EHL). Ankle everters included peroneus longus (PL) and peroneus brevis (PB). These functional groups were defined to compare muscle architectural measures and fiber type distributions across joints.

Comparisons were also made between muscles that served primarily an anti-gravity function and those that did not. The anti-gravity muscles were GSup, GMed, muscle X, VI, VL, VM, RF, GLH, GMH, SOL, PLA, TP, FDL and FHL. Remaining muscles were considered non-anti-gravity muscles.

There are several muscles in the rat hindlimb that are widely studied in laboratories, which we have defined as 'typical' muscles. This was important in order to determine whether 'typical' muscles really are representative of the entire hindlimb. These muscles included VL, GLH, GMH, SOL, PLA, TA and EDL.

### Statistical analysis

All values are reported as mean ± standard error (s.e.m.) unless otherwise noted. Independent sample *t*-tests were used to compare architectural variables from typical rat muscles to the other muscles in the hindlimb and to make functional group comparisons. One-way repeated measures analyses of variance (ANOVA) was used to test for architectural and fiber type differences among the typically studied rat muscles. *Post-hoc* pairwise comparisons (with Tukey's *post-hoc* corrections) were made for variables after finding a significant one-way ANOVA.

PCSA was calculated using two measures made directly on the muscles: mass and fiber length. To determine which of these two measures drives the PCSA value, multiple stepwise regression was used to determine the relative contributions of fiber length and mass to PCSA.

Discriminant analysis was performed to investigate differences in architectural and fiber type parameters between functional muscle groups within the rat hindlimb. Grouping variables included joint, anti-gravity *versus* non-anti-gravity muscles, and functional muscle groups. Architectural data and fiber type data from contralateral limbs were combined based on the assumption that minimal differences should exist between limbs. Discriminant analysis was performed on the rat hindlimb dataset using the following variables: mass, muscle length, fiber length, PCSA, $L_f/L_m$ ratio, fiber type I percentage, type IIA percentage, type IIX percentage and type IIB percentage.

To examine architectural patterns across species, discriminant analysis was also used to predict species or muscle, given either absolute or relative architectural parameters. The species examined were the mouse ($N$=8) (Burkholder et al., 1994), rat ($N$=6), cat ($N \leqslant 4$) (Sacks and Roy, 1982), human ($N$=19) (Ward et al., in press), and horse ($N$=7) (Payne et al., 2005). Because complete data sets from the cat and horse were not available, muscle architectural variables were averaged across individual specimens for each species.

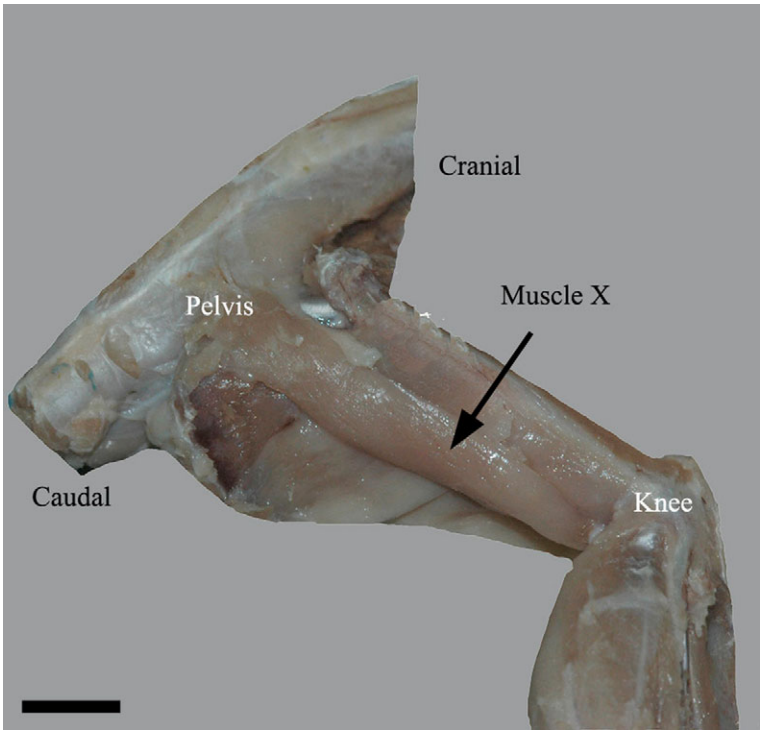


Fig. 1. Lateral view of a rat hindlimb transected above the lumbar spine, with muscle X indicated by the arrow. The origin of the muscle is on the craniolateral pelvis and its insertion on the craniomedial tibia. Scale bar, 10 mm.

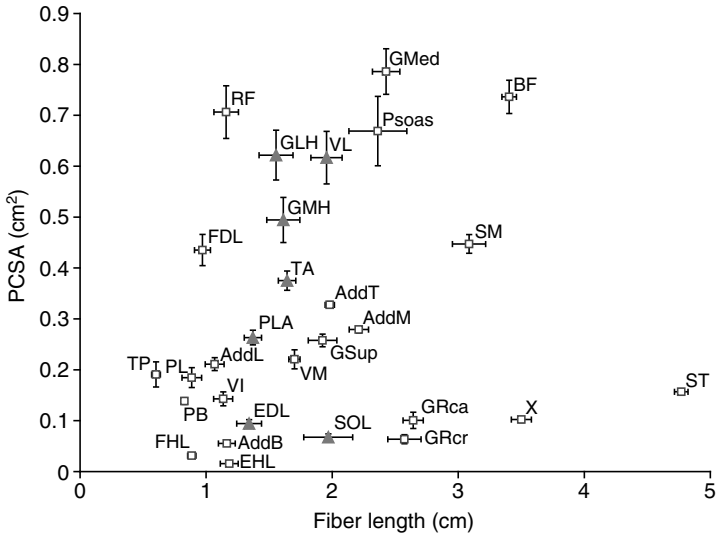


Fig. 2. Scatter plot of fiber length and physiological cross-sectional area (PCSA) in the muscles of the rat hindlimb. Muscles included psoas, gluteus superficialis (GSup), gluteus medius (GMed), adductor brevis (AddB), adductor longus (AddL), adductor magnus (AddM), adductor tertius (AddT), rectus femoris (RF), vastus intermedius (VI), vastus lateralis (VL), vastus medialis (VM), biceps femoris (BF), semitendinosus (ST), semimembranosus (SM), muscle X, cranial head of gracilis (GRcr), caudal head of gracilis (GRca), medial head of gastrocnemius (GMH), lateral head of gastrocnemius (GLH), plantaris (PLA), soleus (SOL), tibialis posterior (TP), flexor digitorum longus (FDL), flexor hallucis longus (FHL), peroneus longus (PL), peroneus brevis (PB), tibialis anterior (TA), extensor digitorum longus (EDL), and extensor hallucis longus (EHL). Typically studied rat muscles are represented by filled triangles; all other muscles are represented by open squares.

Table 1. Architectural properties of muscles and functional groups in the rat hindlimb

| Muscle ($N$=6) | Mass (mg) | Muscle length (cm) | Fiber length (cm) | Pennation angle (deg.) | PCSA (cm$^2$) | $L_f/L_m$ |
|---|---|---|---|---|---|---|
| Psoas | 1784.83±296.10 | 5.55±0.26 | 2.36±0.23 | 17.1±0.8 | 0.67±0.07 | 0.42±0.02 |
| Glut. superficialis† | 521.00±31.66 | 2.55±0.17 | 1.92±0.11 | –1.1±0.7 | 0.26±0.01 | 0.56±0.03 |
| Glut. medius† | 1992.33±47.38 | 3.64±0.16 | 2.43±0.11 | 0.6±0.8 | 0.79±0.05 | 0.67±0.05 |
| Muscle X† | 377.00±17.21 | 4.31±0.12 | 3.50±0.08 | 1.0±1.0 | 0.10±0.01 | 0.81±0.01 |
| Rectus femoris† | 945.33±33.23 | 3.21±0.11 | 1.16±0.10 | 25.4±4.0 | 0.71±0.05 | 0.36±0.04 |
| Vastus lateralis*,† | 1288.83±41.22 | 3.42±0.08 | 1.96±0.12 | 10.0±3.3 | 0.62±0.05 | 0.57±0.04 |
| Vastus intermedius† | 170.67±15.53 | 2.64±0.16 | 1.14±0.08 | 6.9±1.2 | 0.14±0.01 | 0.44±0.04 |
| Vastus medialis† | 442.50±44.81 | 2.79±0.09 | 1.70±0.04 | 24.7±3.4 | 0.22±0.02 | 0.61±0.02 |
| Gracilis cranial head | 173.00±27.68 | 3.04±0.15 | 2.57±0.13 | 0.0±0.0 | 0.06±0.01 | 0.84±0.01 |
| Gracilis caudal head | 276.00±38.68 | 3.47±0.14 | 2.64±0.08 | 0.0±0.0 | 0.10±0.02 | 0.76±0.02 |
| Adductor longus | 235.50±11.86 | 1.62±0.06 | 1.07±0.08 | 4.2±1.7 | 0.21±0.01 | 0.66±0.04 |
| Adductor brevis | 66.83±3.26 | 1.57±0.09 | 1.16±0.07 | 0.0±0.0 | 0.06±0.00 | 0.75±0.02 |
| Adductor magnus | 649.83±16.49 | 2.98±0.09 | 2.21±0.08 | 0.0±0.0 | 0.28±0.01 | 0.74±0.02 |
| Adductor tertius | 685.17±18.37 | 2.47±0.07 | 1.98±0.04 | 0.6±0.6 | 0.33±0.01 | 0.80±0.02 |
| Biceps femoris | 2670.83±95.48 | 5.10±0.08 | 3.40±0.06 | 3.6±3.5 | 0.74±0.03 | 0.67±0.02 |
| Semitendinosus | 789.83±33.17 | 5.95±0.09 | 4.77±0.05 | 0.0±0.0 | 0.16±0.02 | 0.80±0.01 |
| Semimembranosus | 1452.83±39.84 | 4.27±0.12 | 3.09±0.13 | 2.1±2.0 | 0.45±0.02 | 0.72±0.02 |
| Tibialis anterior* | 662.17±17.70 | 2.91±0.04 | 1.64±0.07 | 12.8±1.2 | 0.38±0.02 | 0.57±0.03 |
| Extensor hallucis longus | 19.50±0.67 | 1.74±0.09 | 1.18±0.07 | 5.7±1.6 | 0.02±0.00 | 0.68±0.02 |
| Extensor digitorum longus* | 131.83±3.24 | 2.81±0.09 | 1.34±0.10 | 9.0±1.1 | 0.09±0.01 | 0.48±0.05 |
| Peroneus longus | 177.50±7.01 | 2.76±0.04 | 0.89±0.08 | 20.0±3.1 | 0.19±0.02 | 0.32±0.03 |
| Peroneus brevis | 124.67±4.45 | 2.92±0.11 | 0.82±0.02 | 12.6±2.8 | 0.14±0.01 | 0.28±0.01 |
| Gastrocnemius MH*,† | 849.17±24.18 | 3.61±0.06 | 1.61±0.13 | 14.0±3.9 | 0.49±0.04 | 0.45±0.04 |
| Gastrocnemius LH*,† | 1031.17±30.53 | 3.42±0.08 | 1.56±0.14 | 14.2±3.6 | 0.62±0.05 | 0.46±0.05 |
| Soleus*,† | 134.67±4.57 | 2.83±0.19 | 1.97±0.19 | 3.9±2.4 | 0.07±0.01 | 0.69±0.04 |
| Flexor hallucis longus† | 29.67±1.69 | 1.81±0.19 | 0.89±0.03 | 7.5±2.1 | 0.03±0.00 | 0.51±0.04 |
| Flexor digitorum longus† | 463.83±10.87 | 3.22±0.05 | 0.97±0.06 | 19.3±1.9 | 0.44±0.03 | 0.30±0.02 |
| Tibialis posterior† | 135.83±9.71 | 2.67±0.01 | 0.60±0.04 | 26.0±7.3 | 0.19±0.03 | 0.23±0.01 |
| Plantaris*,† | 397.50±16.87 | 4.08±0.07 | 1.37±0.07 | 16.4±3.2 | 0.26±0.01 | 0.34±0.02 |
| Hip flexors | 1365.08±419.75 | 4.38±1.17 | 1.76±0.60 | 21.25±4.17 | 0.69±0.02 | 0.39 ±0.03 |
| Hip extensors† | 1300.64±369.73 | 4.30±0.48 | 3.19±0.40 | 1.02±0.67 | 0.41±0.10 | 0.74±0.03 |
| Hip abductors | 1256.67±735.67 | 3.09±0.54 | 2.18±0.25 | –0.28±0.83 | 0.52±0.26 | 0.72±0.04 |
| Hip adductors | 402.30±118.84 | 2.42±0.37 | 1.28±0.39 | 0.94±0.81 | 0.20±0.05 | 0.75±0.03 |
| Knee flexors | 890.81±261.32 | 4.14±0.31 | 2.72±0.37 | 5.69±2.33 | 0.33±0.08 | 0.65±0.06 |
| Knee extensors† | 711.83±250.48 | 3.01±0.18 | 1.49±0.20 | 16.77±4.83 | 0.42±0.14 | 0.50±0.06 |
| Plantarflexors† | 371.56±117.83 | 3.04±0.22 | 1.19±0.15 | 14.88±2.21 | 0.27±0.07 | 0.40±0.05 |
| Dorsiflexors | 271.17±15.90 | 2.49±0.38 | 1.39±0.13 | 9.17±2.05 | 0.16±0.11 | 0.58±0.06 |

*'Typical' rat hindlimb muscles (see text).

†Anti-gravity muscles.

Values are means ± s.e.m.

$L_f$, fiber length normalized to a sarcomere length of 2.4 μm; $L_m$, muscle length normalized to a sarcomere length of 2.4 μm; PSCA, physiological cross-sectional area.

Table 2. Myosin heavy chain isoform percentages in muscles and functional groups in the rat hindlimb

| Muscle (*N*=6) | Myosin heavy chain isoform | | | |
|---|---|---|---|---|
| | I (%) | IIa (%) | IIx (%) | IIb (%) |
| Psoas | 2.05±1.34 | 11.03±0.95 | 22.76±1.57 | 64.16±2.59 |
| Glut. superficialis† | 0.00±0.00 | 10.76±1.58 | 24.51±1.92 | 64.72±3.35 |
| Glut. medius† | 0.00±0.00 | 5.22±0.62 | 19.01±0.59 | 75.77±0.13 |
| Muscle X† | 0.00±0.00 | 5.34±1.71 | 25.26±1.95 | 69.40±0.70 |
| Rectus femoris† | 1.09±0.35 | 9.29±0.65 | 28.12±2.09 | 61.51±2.07 |
| Vastus lateralis*,† | 1.24±0.80 | 12.36±1.81 | 21.82±0.71 | 64.58±2.37 |
| Vastus intermedius† | 25.71±2.56 | 19.54±1.59 | 25.89±1.49 | 28.87±3.65 |
| Vastus medialis† | 6.19±1.14 | 13.00±1.53 | 22.36±0.95 | 58.44±2.99 |
| Gracilis cranial head | 7.82±0.70 | 10.71±0.82 | 22.08±1.81 | 59.40±2.81 |
| Gracilis caudal head | 11.36±0.34 | 9.99±1.23 | 20.86±0.91 | 57.79±1.70 |
| Adductor longus | 2.91±1.90 | 0.00±0.00 | 39.54±1.54 | 57.54±2.31 |
| Adductor brevis | 49.33±3.62 | 13.97±0.77 | 20.29±2.60 | 16.42±2.84 |
| Adductor magnus | 0.00±0.00 | 0.00±0.00 | 17.36±1.09 | 82.64±1.09 |
| Adductor tertius | 1.20±0.55 | 6.09±0.32 | 24.06±1.14 | 68.64±1.16 |
| Biceps femoris | 0.00±0.00 | 6.55±0.58 | 16.42±0.39 | 77.03±0.59 |
| Semitendinosus | 3.39±0.72 | 8.45±1.05 | 19.26±0.87 | 68.90±1.67 |
| Semimembranosus | 0.00±0.00 | 6.47±0.57 | 14.82±0.91 | 78.72±0.84 |
| Tibialis anterior* | 0.43±0.43 | 10.13±0.64 | 19.69±0.65 | 69.75±0.90 |
| Extensor hallucis longus | 1.16±1.16 | 0.00±0.00 | 54.82±1.81 | 44.03±2.69 |
| Extensor digitorum longus* | 0.00±0.00 | 10.53±0.40 | 25.08±1.40 | 64.40±1.33 |
| Peroneus longus | 11.09±1.11 | 23.15±1.26 | 42.45±1.21 | 23.32±1.54 |
| Peroneus brevis | 1.68±1.09 | 0.00±0.00 | 72.19±1.84 | 26.13±1.95 |
| Gastrocnemius MH*,† | 5.71±0.33 | 9.80±1.07 | 19.01±0.59 | 63.53±1.52 |
| Gastrocnemius LH*,† | 6.81±0.64 | 7.90±0.67 | 24.51±1.92 | 57.41±2.85 |
| Soleus*,† | 80.19±4.10 | 19.81±4.10 | 0.00±0.00 | 0.00±0.00 |
| Flexor hallucis longus† | 7.81±0.82 | 1.09±1.09 | 65.70±2.02 | 25.40±1.92 |
| Flexor digitorum longus† | 6.89±1.31 | 16.13±1.66 | 42.36±3.19 | 34.63±2.77 |
| Tibialis posterior† | 3.36±1.11 | 11.01±0.55 | 36.98±2.64 | 48.65±2.65 |
| Plantaris*,† | 4.83±0.59 | 11.31±0.72 | 38.25±1.53 | 45.61±1.60 |
| Hip flexors | 1.57±0.48 | 10.16±0.87 | 25.44±2.68 | 62.83±1.33 |
| Hip extensors† | 0.56±0.56 | 7.13±0.87 | 19.88±1.72 | 72.42±2.26 |
| Hip abductors | 0.00±0.00 | 7.99±2.77 | 21.76±2.75 | 70.25±5.52 |
| Hip adductors | 12.75±9.32 | 6.00±2.75 | 24.57±3.90 | 56.68±11.05 |
| Knee flexors | 4.44±1.33 | 8.50±0.70 | 22.27±2.30 | 64.20±3.50 |
| Knee extensors† | 8.56±5.84 | 13.55±2.16 | 24.55±1.49 | 53.35±8.26 |
| Plantarflexors† | 14.26±8.29 | 11.13±2.59 | 37.94±7.42 | 36.07±6.60 |
| Dorsiflexors | 0.53±0.34 | 6.89±3.44 | 33.19±10.92 | 59.39±7.84 |

Values are means ± s.e.m.
*'Typical' rat hindlimb muscles (see text).
†Anti-gravity muscles.

Absolute architectural variables used were fiber length, mass and PCSA. Relative architectural variables included ($L_f/L_m$ ratio) and PCSA relative to VL mass (PCSA/VLmass).

Scaling of muscle architecture with body mass ($M$) across species was examined using least squares regression of log-transformed variables. Body mass was treated as the independent variable and the architectural variable was the dependent variable. The coefficient and exponent of the allometric equation, $y=aM^b$ (where $y$ is the architectural variable, $a$ is the coefficient, $M$ is body mass, and $b$ is the scaling exponent) were used to compare scaling relationships among hindlimb muscles. Statistical tests were performed using SPSS software (SPSS, Inc., Version 11.5, Chicago, IL, USA). Significance was set at the $P<0.05$ level.

Table 3. Multiple regression of fiber length and mass with physiological cross-sectional area

| Variable | Model 1 | | | Model 2 | | |
|---|---|---|---|---|---|---|
| | B | *s.e.* B | β | B | *s.e.* B | β |
| Mass | 0.313 | 0.014 | 0.859 | 0.384 | 0.013 | 1.054 |
| Fiber length | | –0.010 | 0.001 | –0.386 | | |
| $R^2$ | 0.738 | 0.850 | | | | |
| $F$ for change in $R^2$ | 479.72* | 125.33* | | | | |

*$P<0.001$.

## RESULTS

### Individual muscles of the rat hindlimb

The total number of muscles examined was 174 (29 muscles from six rats), comprising 60 hip muscles, 42 knee muscles and 72 ankle muscles. Of these muscles 50.6% served an anti-gravity function and 49.4% did not. A survey of the muscles reveals a wide variety of functional specializations in the rat hindlimb (Fig. 2, Table 1). For example, ST and GR, with their long fibers and small PCSAs, are designed to generate large excursion or velocity, with a low capacity for force generation. Conversely, muscles such as RF, VL, GLH and GMH, with large PCSAs and short fibers are predicted to generate large forces over a short distance. Muscles that fall in the middle of these two extremes were not biased toward either excursion or force production (i.e. SM, AddT and AddM). Examination of the fiber type composition of the two muscles at the architectural extremes, RF (short fibers and large PCSA) and ST (long fibers and small PCSA), demonstrates that these muscles do not show dramatic differences in fiber type composition (Table 2). Although both muscles are composed of less than 5% type I fibers, there is a relatively modest difference in the type II fiber isoforms (<10%), suggesting that a muscle that is architecturally fast need not be biochemically fast. This theme was observed for a number of other muscles as well (cf. Fig. 2 and Table 2).

The muscles of the rat hindlimb span an eightfold range of fiber lengths, from 0.60 cm in TP to 4.77 cm in ST (Fig. 2, Table 1). PCSA, however, spans a 40-fold range, from 0.02 $cm^2$ in EHL to 0.79 $cm^2$ in GMed. Multiple stepwise regression confirmed that, in the rat hindlimb, mass is the major determinant of PCSA (Table 3). When fiber length is added to the regression equation, it increases the $R^2$ from 0.738 to 0.850 indicating that rat muscles increase their power largely by increasing their mass rather than changing the length of their fibers.

Although hamstring muscles had longer fiber lengths, in the range of 3.09 cm (SM) to 4.77 cm (ST), most of the rat muscles were biased towards shorter fibers, with 63% of muscles examined having fibers shorter than 2.0 cm. In addition to fiber length, fiber-length-to-muscle-length ratio ($L_f/L_m$) is an indicator of a muscle's potential to generate excursion that is independent of muscle size (Table 1). More proximal muscle groups (excluding hip flexors) tended to have higher $L_f/L_m$ ratios than distal muscle groups. Biarticular muscles (e.g. muscle X, GR and the hamstring muscles) had higher $L_f/L_m$

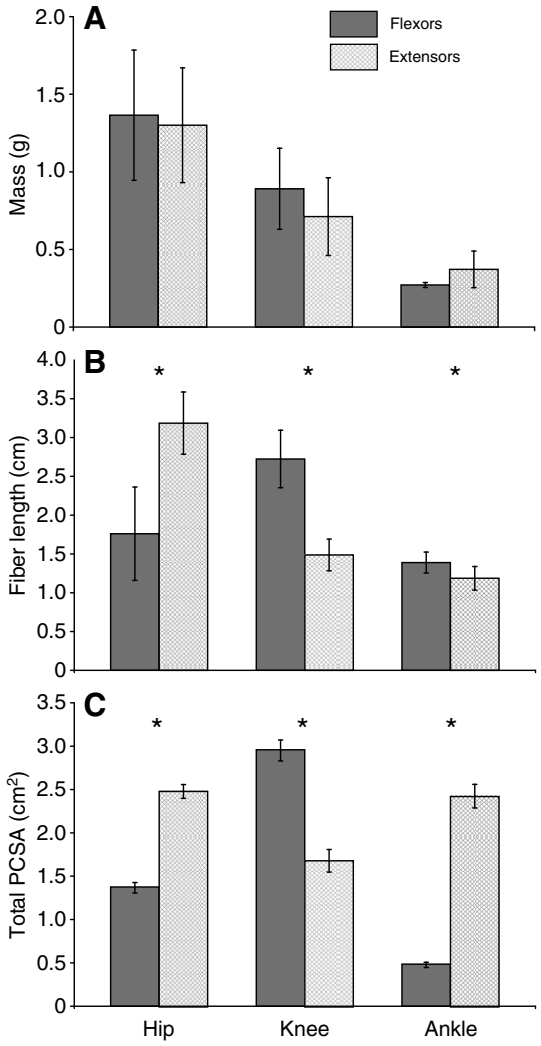


Fig. 3. Comparison of mass (A), fiber length (B) and total physiological cross-sectional area (PCSA; C) across functional muscle groups in the rat hindlimb. Flexors at the hip, knee and ankle are shown as solid bars, whereas the extensors are shown as hatched bars. The functional groups include hip flexors ($N$=2 muscles), hip extensors ($N$=6), knee flexors ($N$=9), knee extensors ($N$=4), dorsiflexors ($N$=3) and plantarflexors ($N$=9). *Significant difference between muscle groups at each joint ($P$<0.05).

ratios than muscles that only crossed a single joint. Three exceptions were the GLH, GMH and PLA. The need for force generation in these important anti-gravity muscles may be greater than the need to generate a large range of motion. Other anti-gravity muscles had similarly low $L_f/L_m$ ratios, consistent with their need to generate large forces.

With regard to fiber type, almost all rat hindlimb muscles would be considered 'fast'. Across all muscles except SOL, type IIB was the most prevalent isoform. Many muscles were so biased towards the faster phenotype that they did not contain a detectable level of the type I MHC (Table 2). Architecturally, the mean PCSA of the 'typically studied' muscles (0.36±0.03 cm$^2$) was not significantly different from the mean PCSA for all muscles (0.29±0.02 cm$^2$; $P$>0.05; Table 1). The average fiber length of the typically studied muscles (1.64±0.06 cm) was significantly shorter than the average fiber length of the remaining rat hindlimb muscles (1.92±0.10 cm; $P$<0.05). Thus, the range of fiber lengths found in the rat hindlimb is not represented by these typically studied muscles (Fig. 2).

### Functional muscle groups

Examining architectural and fiber type properties of muscles grouped according to function provide further evidence of functional specialization in the muscles of the rat hindlimb. Muscle mass, fiber length, and total PCSA varied considerably among muscle groups (Fig. 3A–C). In general, proximal muscles had the largest masses (Fig. 3A) whereas hip and knee muscle groups, containing larger numbers of biarticular muscles (hip extensors and knee flexors), had the longest fiber lengths (Fig. 3B; $P$<0.05). Plantarflexors had significantly shorter fibers compared with dorsiflexors ($P$<0.05). Because these two functional groups have similar mass, this architectural specialization enables plantarflexors to achieve larger PCSA, and in turn, more force. Hip extensors and ankle plantarflexors had larger PCSA compared to hip flexors and ankle dorsiflexors (Fig. 3C), consistent with their anti-gravity function and the large number of muscles in these groups ($P$<0.05). Knee flexors had a larger PCSA compared with knee extensors, because of the large number of muscles in this group ($P$<0.05).

An important fiber type difference between muscle groups was observed at the ankle, where plantarflexors had a significantly higher percentage of type I and IIA muscle fibers compared with dorsiflexors ($P$<0.05), consistent with their anti-gravity function (Fig. 4). The differences in fiber type percentages between plantarflexors and dorsiflexors were significant even with the exclusion of SOL with its high type I percentage. Thus, the differences in fiber type were not driven by one muscle but were consistent across the plantarflexor group. When muscles were grouped according to anti-gravity function, anti-gravity muscles had a significantly higher percentage of type IIA muscle fibers and a significantly lower percentage of type IIB muscle fibers ($P$<0.05) than their antagonists.

### The rat hindlimb as a model

Discriminant analysis confirmed that significant architectural and fiber type specialization exists across joints, anti-gravity muscles, and functional groups. Specifically, discriminant analysis confirmed that architectural parameters are the most important predictors of anatomy (i.e. joint) as well as function (i.e. anti-gravity muscles, primary muscle action). $L_f/L_m$ ratio, mass, fiber length and muscle length were the most important discriminators of the primary joint over which a muscle acted, followed by type IIB and then type IIA percentage (Table 4). The discriminating function was able to correctly identify the joint over which a muscle acted in 73% of the cases (compared to 33% by chance).

Analysis using functionally relevant grouping variables discriminated between groups with greater accuracy. For example, the following parameters were significant discriminators between anti-gravity and non anti-gravity muscles: $L_f/L_m$ ratio, type IIA percentage, PCSA and mass (Table 5). Using this discriminating function, group membership was correctly identified in 76% of the cases. When muscles were grouped according to their primary action in the hindlimb, the predictive architectural and fiber type parameters were fiber length, muscle length, $L_f/L_m$ ratio, type IIB percentage, mass, PCSA and type IIA percentage, which correctly identified group membership in 70% of cases (Table 6). Thus, fiber type plays a more important role in determining group membership when function is considered. However, architectural properties still had the greatest discriminating power, with $F$-values consistently higher than those of the fiber type parameters in all discriminant functions.

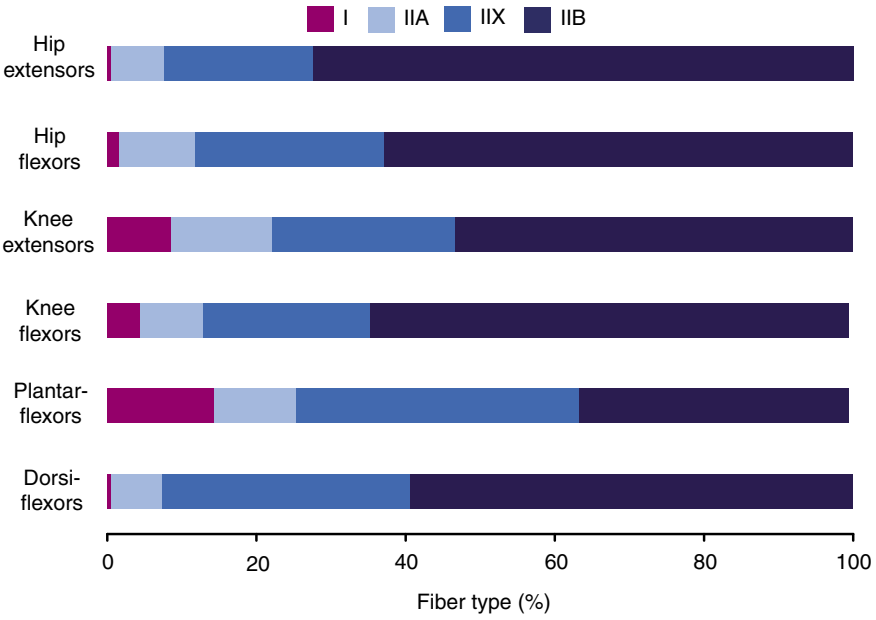


Fig. 4. Comparison of myosin heavy chain isoform percentages for each functional muscle group (color coded, see key) in the rat hindlimb.

Although $L_f/L_m$ ratio and PCSA were common predictors of group membership in several of our analyses, these two parameters did not co-vary significantly with one another.

### Interspecies comparisons

When using absolute architectural variables, species predictors were PCSA, fiber length and mass (Table 7). Using this discriminant function, the species of interest was correctly classified in 53% of cases (20% of the cases could be expected to be correctly identified by chance alone). The species used in the analysis varied in body mass by 2000-fold (e.g. $M_{horse}$~500 kg and $M_{mouse}$~25 g). Therefore, it is not surprising that the absolute measures that vary with body mass were useful predictors of the species of interest. Relative architectural measures that predicted species were PCSA/VL mass and $L_f/L_m$ ratio (Table 7). PCSA/VL mass was a stronger predictor of species, and therefore, relative force-generating capacity may be more variable across species than relative excursion. These measures correctly identified species in 44% of cases.

The relative fiber lengths of several leg muscles (GLH, GMH, FDL, TA and EDL) and one hip muscle (AddL) scaled negatively with body mass (Table 8). There was a large range of scaling exponents, from –0.06 in adductor longus to –0.17 in soleus

Table 4. Discriminant analysis of rat hindlimb muscles using primary joint as the grouping variable

| Step | Variable entered | Wilks' lambda | *F*-statistic |
|---|---|---|---|
| 1 | $L_f/L_m$ ratio | 0.614 | 52.74* |
| 2 | Mass | 0.489 | 35.93* |
| 3 | Fiber length | 0.453 | 26.85* |
| 4 | Muscle length | 0.375 | 26.07* |
| 5 | IIB fiber percentage | 0.352 | 22.50* |
| 6 | IIA fiber percentage | 0.331 | 20.07* |

*$P$<0.05.
$L_f/L_m$, fiber length to muscle length.

Table 5. Discriminant analysis of antigravity and non-antigravity muscles in the rat hindlimb

| Step | Variable entered | Wilks' lambda | *F*-statistic |
|---|---|---|---|
| 1 | Fiber length | 0.342 | 48.71* |
| 2 | Muscle length | 0.138 | 42.48* |
| 3 | $L_f/L_m$ ratio | 0.080 | 33.92* |
| 4 | IIB percentage | 0.053 | 28.73* |
| 5 | Mass | 0.038 | 25.07* |
| 6 | PCSA | 0.028 | 22.77* |
| 7 | IIA fiber percentage | 0.023 | 20.17* |

*$P$<0.05.
$L_f/L_m$, fiber length to muscle length; PCSA, physiological cross-sectional area.

Table 6. Discriminant analysis of rat hindlimb muscles using functional group as the grouping variable

| Step | Variable entered | Wilks' Lambda | *F*-statistic |
|---|---|---|---|
| 1 | Fiber length | 0.342 | 48.71* |
| 2 | Muscle length | 0.138 | 42.48* |
| 3 | $L_f/L_m$ ratio | 0.080 | 33.92* |
| 4 | IIB percentage | 0.053 | 28.73* |
| 5 | Mass | 0.038 | 25.07* |
| 6 | PCSA | 0.028 | 22.77* |
| 7 | IIA fiber percentage | 0.023 | 20.17* |

*$P$<0.05.
$L_f/L_m$, fiber length to muscle length; PCSA, physiological cross-sectional area.

Table 7. Discriminant analysis of hindlimb muscles using species as the grouping variable and absolute architectural variables (function 1) and relative architectural variables (function 2) as the predictors

| Function | Step | Variable entered | Wilks' Lambda | *F*-statistic |
|---|---|---|---|---|
| 1 | 1 | PCSA | 0.45 | 24.99* |
| | 2 | Fiber length | 0.28 | 17.89* |
| | 3 | Mass | 0.24 | 12.85* |
| 2 | 1 | $L_f/L_m$ ratio | 0.76 | 6.58* |
| | 2 | PCSA/VL mass | 0.56 | 16.42* |

*$P$<0.05.
$L_f/L_m$, fiber length to muscle length; PCSA, physiological cross-sectional area; VL, vastus lateralis.

Table 8. Scaling relationship of fiber length to muscle length ratio ($L_f/L_m$ ratio) and body mass for mouse, rat, cat, human and horse hindlimb muscles

| Muscle | *b* | *a* | $R^2$ |
|---|---|---|---|
| AddL‡ | –0.06 | 0.004 | 0.95* |
| RF | –0.06 | –0.33 | 0.51 |
| VL | –0.05 | –0.20 | 0.27 |
| VM | –0.08 | –0.14 | 0.53 |
| VI | –0.05 | –0.28 | 0.40 |
| GR | –0.06 | 0.08 | 0.54 |
| BF | –0.03 | –0.14 | 0.12 |
| ST | 0.00 | –0.13 | 0.00 |
| SM | –0.09 | 0.08 | 0.48 |
| GLH | –0.08 | –0.21 | 0.83* |
| GMH | –0.10 | –0.19 | 0.86* |
| SOL | –0.17 | 0.17 | 0.73† |
| PLA‡ | 0.03 | –0.57 | 0.07 |
| TP | –0.12 | –0.25 | 0.60† |
| FDL | –0.11 | –0.27 | 0.85* |
| FHL‡ | –0.08 | –0.31 | 0.35 |
| TA | –0.16 | –0.13 | 0.79* |
| EDL | –0.08 | –0.16 | 0.84* |
| All muscles | –0.07±0.01 | | |
| Proximal muscles | –0.05±0.01 | | |
| Distal muscles | –0.10±0.02 | | |
| Plantarflexors | –0.09±0.02 | | |
| Dorsiflexors | –0.12±0.04 | | |
| Hamstrings | –0.04±0.03 | | |
| Quadriceps | –0.06±0.01 | | |

*$P$<0.05; †0.05<$P$<0.13.
‡Horse not included in muscle data set.
Scaling equation is in the form $y=aM^b$ where $M$ is body mass. $R^2$ is shown for the line describing the relationship between log-transformed variables. Scaling exponents for muscle groups are shown (mean ± s.e.m.).
For muscle names see text.

Table 9. Scaling relationship of the ratio of physiological cross-sectional area to vastus lateralis mass (PCSA/VL mass) and body mass for mouse, rat, cat, human and horse hindlimb muscles

| Muscle | *b* | *a* | $R^2$ |
|---|---|---|---|
| AddL‡ | –0.39 | 0.05 | 0.90* |
| RF | –0.30 | 0.48 | 0.80* |
| VL | –0.29 | 0.44 | 0.99* |
| VM | –0.23 | 0.04 | 0.79* |
| VI | –0.19 | –0.44 | 0.96* |
| GR | –0.08 | –1.10 | 0.10 |
| BF | –0.47 | 0.91 | 0.94* |
| ST | –0.34 | 0.14 | 0.84* |
| SM | –0.15 | –0.41 | 0.59† |
| GLH | –0.32 | 0.44 | 0.83* |
| GMH | –0.28 | 0.35 | 0.91* |
| SOL | 0.04 | –1.22 | 0.06 |
| PLA‡ | –0.56 | 0.61 | 0.78† |
| TP | –0.12 | –0.79 | 0.44 |
| FDL | –0.25 | 0.00 | 0.37 |
| FHL‡ | –0.26 | –0.28 | 0.35 |
| TA | –0.30 | 0.11 | 0.87* |
| EDL | –0.19 | –0.64 | 0.81* |
| All muscles | –0.26±0.03 | | |
| Proximal muscles | –0.27±0.04 | | |
| Distal muscles | –0.25±0.05 | | |
| Plantarflexors | –0.25±0.07 | | |
| Dorsiflexors | –0.24±0.06 | | |
| Hamstrings | –0.32±0.09 | | |
| Quadriceps | –0.25±0.03 | | |

*$P$<0.05; †0.05<$P$<0.13.
‡Horse not included in muscle data set.
Scaling equation is in the form $Y=aM^b$ where $M$ is body mass. $R^2$ is shown for the line describing the relationship between log-transformed variables. Scaling exponents for muscle groups are shown (means ± s.e.m.).
For muscle names, see text.

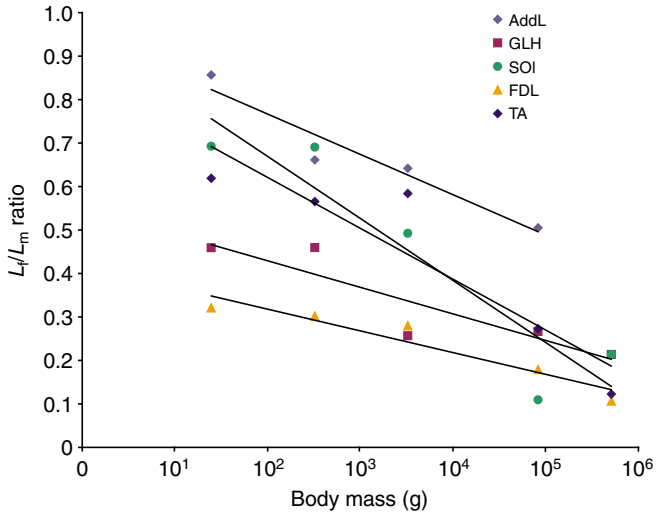


Fig. 5. Semi log-transformed plot of relationship of fiber-length-to-muscle-length ratio ($L_f/L_m$ ratio) and body mass in adductor longus (AddL), lateral head of gastrocnemius (GLH), soleus (SOL), flexor digitorum longus (FDL) and tibialis anterior (TA). The $L_f/L_m$ ratio of all muscles scales negatively with increasing body mass, meaning that larger animals generate relatively smaller fiber excursions than smaller animals. This is especially true for the TA and SOL, both of which have larger scaling exponents than the other muscles.

(Fig. 5). Relative PCSA showed a significant scaling relationship with body size in both proximal and distal muscles (Table 9).

## DISCUSSION

The purpose of this study was to define the architectural and fiber type properties of the rat hindlimb in order to study muscle design. Using discriminant analysis, we demonstrated that the key design features of a muscle are its PCSA and fiber length, with fiber type distribution being important when comparing muscles within functional groups. This was primarily illustrated by the fact that variation in architectural parameters among functional groups was of almost two orders of magnitude whereas fiber type variation was typically only about 25%.

The anti-gravity status of a muscle influences its architectural properties and fiber type. Force generation to support an individual's body weight against the load of gravity is the primary determinant of the metabolic cost of locomotion (Kram and Taylor, 1990). In addition to their importance in movement, anti-gravity muscles also must be used to maintain an upright posture while the individual is static. The maintenance of static postural stability would be best performed with slow fibers that resist fatigue. Thus, we expected the anti-gravity status to influence functional demands placed on a muscle and therefore the design parameters of the muscle. Our results confirm this hypothesis. Anti-gravity muscles in the rat have a greater force-generating capacity (reflected in the relatively greater PCSAs and smaller fiber length to muscle length ratios, implying that more fibers are packed in parallel in the muscles) than non-

anti-gravity muscles. In terms of fiber type, the anti-gravity muscles had a significantly higher proportion of type IIA fiber and lower proportion of type IIB fibers compared with the non-anti-gravity muscles.

Detailed comparison among functional muscle group architectural properties may be confounded by the fact that muscles have multiple tasks. For example, most knee flexors are also hip extensors and therefore have larger PCSAs than would be expected from a simple non-anti-gravity muscle group. Similarly, hip extensors have much longer fiber lengths than the hip flexors, but this is driven by the fact that a large number of hip extensors are biarticular and need to have longer fibers to operate at two joints.

When comparing the 'typically studied' muscles across the entire hindlimb dataset, we found that they do not represent the full range of muscle fiber length within the hindlimb but are representative of the PCSA and fiber type values observed in rat. The implications of this finding is that studies emphasizing changes in muscle mass or fiber type composition could fairly be deduced from studies of these typical muscles. This represents the majority of the functional studies in the rat. However, studies in which the variation in fiber length is an important parameter (immobilization, length–tension relationships, serial sarcomere number adaptation and series fiber studies) would not accurately represent the range of effects that could be observed in the hindlimb. Of course, specific recommendations for an appropriate model muscle depend on the study proposed, but the architectural data contained herein should be used as a guideline.

This study confirms that rat lower extremity muscles contain a predominance of fast muscle fibers. Therefore, full elucidation of the relationship between muscle architecture and fiber type may not be possible in this animal model. Nonetheless, significant variation in fiber type existed between muscles and this variation may illustrate differing functional requirements between muscles.

Similarly, contractile differences between fast and slow muscle fibers (e.g. maximum contractile velocity) are more pronounced than differences among fast fiber types. Because most rat hindlimb muscles are predominantly composed of fast fibers, functional differences among muscles with different proportions of the fast fiber types will be less pronounced than functional differences based on architecture.

Previous studies have found proximal-to-distal and superficial-to-deep gradients in the relative amount of fast and slow fibers within limbs. Although evidence for regionalization of fiber type has been found within muscles and muscle groups, we were interested in functionally relevant differences between muscles and muscle groups and therefore chose not to pursue this issue in our study.

### Interspecies scaling relationships

Previous work on the scaling of hindlimb muscle architecture with body size has established that different scaling rules apply for proximal and distal muscle groups (Alexander et al., 1981), but a more specific examination of how these rules vary among single muscles has not been undertaken. If it is indeed true that fiber lengths of proximal and distal muscles scale proportional to $M^{0.3}$ and $M^{0.17}$, respectively (Alexander et al., 1981), and muscle length is proportional to bone length, which scales with $M^{0.35}$(Alexander et al., 1979), then the $L_f/L_m$ ratio should scale proportional to $M^{-0.05}$ or $M^{-0.18}$ (in proximal and distal muscles, respectively). Conversely, isometry predicts that the dimensionless fiber-length-to-muscle-length ratio should remain constant with increasing body mass. If PCSA scales proportional to $M^{0.8}$ and VL mass proportional to $M^{1.1}$ (Alexander et al., 1981), then the ratio of PCSA to VL mass should scale proportional to $M^{-0.3}$. This is similar to the scaling exponent predicted by isometry, $M^{-0.33}$ (PCSA/mass=$M^{2/3}/M^{1}$).

When examining scaling of relative fiber length, a significant scaling relationship was found in most leg muscles and one hip muscle. The scaling exponents ranged from –0.06 in AddL to –0.17 in SOL (Fig. 5). This is consistent with the range predicted from previously determined scaling relationships, but the exponents for several distal leg muscles are higher than expected (i.e. EDL, FDL and FHL), implying that relative fiber length in these leg muscles of larger animals is greater than would be predicted. However, it is still the case that relative fiber length scales negatively with increasing body mass, although the disparity in potential excursion of the leg muscles may not be as great as current scaling rules predict. It is interesting to note the range of scaling exponents within single muscle groups. For example, in the ankle dorsiflexors, EDL scales proportional to $M^{-0.08}$ whereas TA scales proportional to $M^{-0.16}$ (Table 8). This implies that EDL relative fiber length will decrease less sharply in larger animals. The maintenance of long fiber lengths in EDL implies that excursion in this muscle is important for producing digital extension during gait whereas TA may be more important for force generation in the anterior compartment. GLH and GMH relative fiber lengths scale proportional to $M^{-0.08}$ and $M^{-0.10}$, respectively. The need for excursion of these biarticular muscles may be greater than the other uniarticular muscles of the leg and therefore relative excursion (i.e. relative fiber length) would be maintained. Alexander et al. (Alexander et al., 1981) suggested that a decrease in fiber length in distal muscles of larger animals and the consequences on joint range of motion would be compensated for with long elastic tendons. If fiber lengths decrease while the muscle mass remains relatively constant as body size increases, a greater number of short fibers can be packed into the muscle to increase its PCSA. With this configuration, if the muscle is acting isometrically, it can generate higher forces and use elastic tendons for energy storage and release providing more efficient muscle-tendon movement in larger animals. This pattern appears to be true for some but not all distal hindlimb muscles and this highlights the need to consider architectural, and by extension, functional differences within muscle groups. Although it was not examined in this study, changes in relative tendon length and joint configuration (e.g. muscle moment arms) are other factors that would influence fiber excursion in different muscles.

The ratio of PCSA to VL mass scales significantly with body mass in both proximal and distal muscles (Table 9). Several muscles deviate from the predicted scaling exponent of –0.3. For example, PLA scales proportional to $M^{-0.56}$, which implies a precipitous drop in relative force that is not surprising in this arguably vestigial muscle in humans. Many proximal muscles have a higher scaling exponent than predicted, such as SM, VI and VM. This means that the relative force-generating capacity of these proximal muscles is greater in larger animals. These results imply a functional specialization occurring within muscle groups in addition to the proximal to distal specialization.

In summary, this study has revealed that the architectural properties of rat hindlimb muscles vary widely, in contrast to smaller variations in muscle fiber type. The most commonly studied rat muscles are representative of maximum force generating capacity but not muscle excursion. Through discriminant analysis, we have demonstrated that architecture properties define the 'uniqueness' of muscles within a species, and fiber types are useful in defining muscles within muscle sub groups. The interspecies architectural scaling relationships are

consistent with previous data, although there is variation between individual muscles within groups.

Each author certifies that his or her institution has waived approval for the protocol for this investigation and that all investigations were conducted in conformity with ethical principles of research. We gratefully acknowledge the National Institutes of Health grants AR40050, HD048501 and HD050837 and the Department of Veterans Affairs.

## REFERENCES

**Alexander, R. and Ker, R.** (1990). The architecture of leg muscles. In *Multiple Muscle Systems: Biomechanics and Movement Organization* (ed. J. Winters and S.-Y. Woo), p. 801. New York: Springer-Verlag.

**Alexander, R., Jayes, A., Maloiy, G. and Wathuta, E.** (1979). Allometry of the limb bones of mammals from shrew (*Sorex*) to elephant (*Loxodonta*). *J. Zool.* **189**, 305-314.

**Alexander, R., Jayes, A., Maloiy, G. and Wathuta, E.** (1981). Allometry of leg muscles of mammals. *J. Zool.* **1981**, 539-552.

**Ariano, M. A., Armstrong, R. B. and Edgerton, V. R.** (1973). Hindlimb muscle fiber populations of five mammals. *J. Histochem. Cytochem.* **21**, 51-55.

**Armstrong, R. B. and Phelps, R. O.** (1984). Muscle fiber type composition of the rat hindlimb. *Am. J. Anat.* **171**, 259-272.

**Bodine, S. C., Roy, R. R., Meadows, D. A., Zernicke, R. F., Sacks, R. D., Fournier, M. and Edgerton, V. R.** (1982). Architectural, histochemical, and contractile characteristics of a unique biarticular muscle: the cat semitendinosus. *J. Neurophysiol.* **48**, 192-201.

**Bodine, S. C., Roy, R. R., Eldred, E. and Edgerton, V. R.** (1987). Maximal force as a function of anatomical features of motor units in the cat tibialis anterior. *J. Neurophysiol.* **6**, 1730-1745.

**Bottinelli, R., Schiaffino, S. and Reggiani, C.** (1991). Force-velocity relations and myosin heavy chain isoform compositions of skinned fibres from rat skeletal muscle. *J. Physiol.* **437**, 655-672.

**Burkholder, T. J., Fingado, B., Baron, S. and Lieber, R. L.** (1994). Relationship between muscle fiber types and sizes and muscle architectural properties in the mouse hindlimb. *J. Morphol.* **220**, 1-14.

**Edgerton, V. R. and Simpson, D. R.** (1969). The intermediate muscle fiber of rats and guinea pigs. *J. Histochem. Cytochem.* **12**, 828-838.

**Gans, C.** (1982). Fiber architecture and muscle function. In *Exercise and Sport Science Reviews*. Vol. 10, pp. 160-207. Lexington, MA: Franklin University Press.

**Kram, R. and Taylor, C. R.** (1990). Energetics of running: a new perspective. *Nature* **346**, 265-267.

**Lieber, R. L. and Fridén, J.** (2000). Functional and clinical significance of skeletal muscle architecture. *Muscle Nerve* **23**, 1647-1666.

**Lieber, R. L., Fazeli, B. M. and Botte, M. J.** (1990). Architecture of selected wrist flexor and extensor muscles. *J. Hand Surg. [Am]* **15A**, 244-250.

**Lutz, G. J., Sirsi, S. R., Shapard-Palmer, S. A., Bremner, S. N. and Lieber, R. L.** (2002). Influence of myosin isoforms on contractile properties of intact muscle fibers from Rana pipiens. *Am. J. Physiol.* **282**, C835-C844.

**Payne, R., Hutchinson, J., Robilliard, J., Smith, N. and Wilson, A.** (2005). Functional specialization of pelvic limb anatomy in horses (*Equus caballus*). *J. Anat.* **206**, 557-574.

**Peter, J. B., Barnard, R. J., Edgerton, V. R., Gillespie, C. A. and Stempel, K. E.** (1972). Metabolic profiles on three fiber types of skeletal muscle in guinea pigs and rabbits. *Biochemistry* **11**, 2627-2733.

**Powell, P. L., Roy, R. R., Kanim, P., Bello, M. and Edgerton, V. R.** (1984). Predictability of skeletal muscle tension from architectural determinations in guinea pig hindlimbs. *J. Appl. Physiol.* **57**, 1715-1721.

**Pullen, A. H.** (1977). The distribution and relative sizes of fibre types in the extensor digitorum longus and soleus muscles of the adult rat. *J. Anat.* **123**, 467-486.

**Reiser, P. J., Moss, R. L., Giulian, G. and Greaser, M. L.** (1985). Shortening velocity in single fibres from adult rabbit soleus muscle is correlated with myosin heavy chain composition. *J. Biol. Chem.* **260**, 9077-9080.

**Roy, R. R., Powell, P. L., Kanim, P. and Simpson, D. R.** (1984). Architectural and histochemical analysis of the semitendinosus muscle in mice, rats, guinea pigs, and rabbits. *J. Morphol.* **181**, 155-160.

**Sacks, R. D. and Roy, R. R.** (1982). Architecture of the hindlimb muscles of cats: functional significance. *J. Morphol.* **173**, 185-195.

**Schiaffano, S., Hanzlkova, V. and Pierobon, S.** (1970). Relations between structure and function in rat skeletal muscle fibers. *J. Cell Biol.* **47**, 107-119.

**Staron, R. and Pette, D.** (1993). The continuum of pure and hybrid myosin heavy chain-based fibre types in rat skeletal muscle. *Histochemistry* **100**, 149-153.

**Staron, R., Kraemer, W., Hikida, R., Fry, A., Murray, J. and Campos, G.** (1999). Fiber type composition of four hindlimb muscles of adult Fisher 344 rats. *Histochem. Cell Biol.* **111**, 117-123.

**Talmadge, R. J. and Roy, R. R.** (1993). Elecrophoretic separation of rat skeletal muscle myosin heavy-chain isoforms. *J. Appl. Physiol.* **75**, 2337-2340.

**ter Keurs, H., Luff, A. and Luff, S.** (1984). Force-sarcomere-length relation and filament length in rat extensor digitorum longus muscle. *Adv. Exp. Med. Biol.* **170**, 511-525.

**Ward, S. R. and Lieber, R. L.** (2005). Density and hydration of fresh and fixed human skeletal muscle. *J. Biomech.* **38**, 2317-2320.

**Ward, S. R., Eng, C. M., Smallwood, L. H. and Lieber, R. L.** (in press). Human leg muscle architecture: implications for function, modeling, and surgery. *Clin. Orthop. Rel. Res.*